 Cytometry 29:328–339 (1997)

8 Color, 10-Parameter Flow Cytometry to Elucidate Complex Leukocyte Heterogeneity

Mario Roederer,* Stephen De Rosa, Rachel Gerstein, Michael Anderson, Martin Bigos, Richard Stovel, Thomas Nozaki, David Parks, Leonore Herzenberg, and Leonard Herzenberg

Department of Genetics, Stanford University, Stanford, California

Received 7 April 1997; Accepted 11 July 1997

We developed the chemistry, instrumentation, and software technologies needed to measure, simultaneously and independently, eight different fluorescent molecules on individual cells. Conjugation of these fluorochromes to monoclonal antibodies is straightforward; all immunofluorescence staining is accomplished with direct stains only. We built a hybrid flow cytometer with eight fluorescence detectors and two light scatter channels, with excitation provided by three spatially separated laser beams emitting at 407 nm, 488 nm, and 595 nm. The fluorescence compensation required to make the data orthogonal is of sufficient complexity that it cannot be performed manually; thus, we use software to compensate the data post hoc, based on data collected from singly stained compensation control samples. In this report, we evaluate the 8 color staining technology. Of the seven fluorochromes other than fluorescein, six have a useful brightness at least as great as fluorescein. Three of the fluorochromes (phycoerythrin, allophycocyanin, and the Cy5 resonance energy tandem of phycoerythrin) are considerably brighter than fluorescein and are useful for detecting antigens expressed at low levels. Finally, we show the power and utility of the 8 color, 10-parameter technology using staining experiments on both human and murine immune systems. Cytometry 29:328–339, 1997. © 1997 Wiley-Liss, Inc.

Key terms: resonance energy transfer; spectral compensation; T cell subsets; pre-B cells; pro-B cells; bone marrow leukocytes; GFP (green fluorescent protein)

The advantages of multicolor flow cytometric analysis are well known; over the past 25 years there has been a continuous desire to analyze simultaneously more parameters of each cell. Nonetheless, developments to increase the number of useful parameters has stagnated over the past 15 years—4 color analysis (first performed in the early 1980s) has been supplanted by 5 color analysis in very few laboratories. Three reasons contribute to this relative lack of progress: 1) the low number of available fluorochrome conjugates; 2) the extreme limitations imposed by extant software, which did not allow for the complex types of analyses and postcollection compensation required by high-order multiparameter collections; and 3) the difficulty in adapting commercial flow cytometry platforms to analyze simultaneously more than four or five fluorescences.

The need for more than 5 color analysis has become very clear. The complexity of the immune system is such that identification of phenotypically (and functionally) homogeneous subsets requires the simultaneous measurement of at least six cell surface antigens. Using peripheral human T cells as an example: a minimum of three antigens are required to identify uniquely T cell lineages (i.e., CD3, CD4, and CD8; all three must be present to resolve the $CD4^-CD8^-$ and $CD4^+CD8^+$ from the single positive T cells). In addition, another three colors are required to identify functionally distinct memory lineages (e.g., CD45RA, CD62L, and CD11a). Unique identification of B cell subsets requires at least three measurements and NK subsets require at least four. Unless subsets are uniquely identified by appropriate multiple markers, comparative functional studies between individuals will be artefactually affected by a differential (and unknown) representation of unresolved, functionally distinct subsets.

High-order multiparametric analysis is also required to combine functional and phenotypic analyses. For instance, the assignment of ''Th1'' or ''Th2'' to a particular cell (or subset) requires not only the phenotypic markers noted above, but also two additional measurements devoted to

Contract grant sponsor: National Institutes of Health; Contract grant numbers: LM-04836, AI-31770, CA-42509.

Portions of these data were reported in the 1996 ISAC meeting, Rimini, Italy, and the 1997 AAI meeting, San Francisco, CA.

*Correspondence to: Mario Roederer, Beckman B011, Stanford, CA 94305-5125.

E-mail: roederer@darwin.stanford.edu

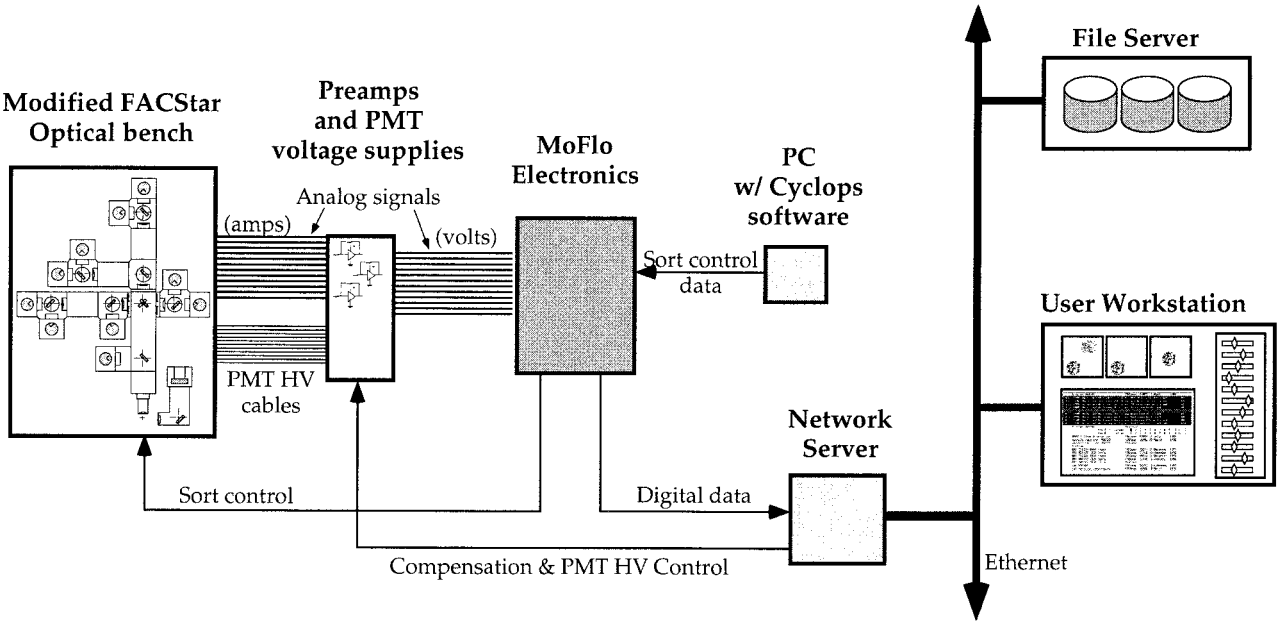

FIG. 1. Diagrammatic layout of the 10-parameter flow cytometer. Our system is a hybrid consisting of a FACStarPlus bench, Cytomation electronics, and our own electronics and computer system. The Cytomation electronics is used to amplify (log or linear mode), evaluate, and digitize the signals from the PMTs. Electronics designed and built in our laboratory allows the computer to set PMT voltages, interface the bench signals to the MoFlo electronics, and handle instrument-to-computer data transfers.

intracellular quantitation of cytokines such as interleukin-4 and γ-interferon. In addition, it is useful to combine other functional measurements such as cell cycle analysis or apoptosis with complete phenotypic identification of cell subsets.

In the past two years, we have made significant advances in the hardware, software, and reagents for flow cytometry analysis. As a result, we have increased our capabilities to the level of seven colors (plus forward and side scatter) with two-laser excitation and eight colors with three-laser excitation. Our reagents include the more commonly-used fluorochromes fluorescein (FITC), phycoerythrin (PE), Cy5PE, Texas Red (TR), allophycocyanin (APC), and Cascade Blue (CB); to this combination we added two relatively new tandem dyes: Cy7PE and Cy7APC. The development and spectral properties of Cy7 tandem dyes for use in immunoglobulin staining experiments has been previously described (23).

Here we describe in detail the development of the 8 color, 10-parameter system. We compare the eight different fluorochrome reagents for use in immunostaining experiments and describe the complex compensation required for analysis. Finally, we show two examples of 8 color staining to demonstrate the power of this approach in dissecting the immune system.

MATERIALS AND METHODS

Antibody Reagents

Unconjugated antibodies were either purified from ascities or tissue culture supernatant or obtained in concentrated form from PharMingen (San Diego, CA). Conjugated antibodies were prepared in our laboratory with the exception of FITC CD8 and Cy5PE RA3-6B2 (PharMingen). Conjugation of all reagents was done as previously described (21).

Cell Staining and Analysis

Human PBMC or mouse bone marrow leukocytes were obtained by standard methods; at least 10^6 cells were used for each stain. Cells were stained on ice for 15 min with fluorescently conjugated antibodies and then washed three times with staining medium (biotin, flavin-deficient RPMI supplemented with 4% newborn calf serum and 0.02% sodium azide). For murine cell analysis, 1 mM EDTA was added to the staining medium to reduce cellular aggregation. Flow cytometry analyses were performed on a hybrid instrument (as described below). Data were collected by FACS-Desk (18) and compensated and analyzed using FlowJo (TreeStar, San Carlos, CA).

Cytometry Hardware

The instrumentation used for this report is a hybrid (Fig. 1). The main optics bench was derived from a FACStarPlus (Becton Dickinson, San Jose, CA). MoFlo electronics (Cytomation, Fort Collins, CO) was used to collect and digitize the data from the ten parameters at 12-bit resolution. Finally, our own electronics was used to control the photomultiplier tube (PMT) voltages, interface the signals from the bench to the MoFlo, and to handle data transfers to the VAX system.

Laser excitation was provided by two primary lasers and a dye head. A 5-watt Innova-90 Argon ion laser (Coherent, Sunnyvale, CA) was run in ''all lines'' mode; a dichroic mirror near the output of this laser reflected part of the

shorter wavelength light (mostly 488 nm) away from the main beam. This beam was filtered to pass only 488 nm light and was steered into the first laser position below the nozzle. The remainder of the ''all lines'' beam was directed into a dye head tuned to 595 nm; the output of the dye laser was steered into the third laser position. Finally, the second laser on the bench was a UV-violet-enhanced Innova-300 Krypton laser (Coherent) operating with 407 nm emission steered into the second laser position below the nozzle. Thus, three parallel but non-colinear beams were used for excitation. Appropriate delay timing was set to collect fluorescences arising from each of the three different excitation beams.

The optical layout was an extension of the standard 5 color layout available on the FACStarPlus (Fig. 2). The primary difference is the presence of three separate apertures, two of which are backed by 45° mirrors, at the focus of the fluorescence signals (Fig. 2, inset). This assembly directs each of the three laser emissions to a different set of photomultiplier tubes (PMTs). The dichroic and interference filters used for each channel are shown in Figure 2. Note the presence of additional relay lenses used in the extended optical layout to ensure proper delivery of light onto the detectors. We used standard PMTs for all detectors except the Cy7 channels, for which we used Hamamatsu R3896 (red-sensitive) PMTs. The R3896 PMTs gave an increase in signal-to-noise of approximately two-fold for Cy7 signals; we found no benefit from using an R636 Gallium-arsenide PMT (data not shown).

RESULTS

Fluorochrome Reagents

The ability to measure simultaneously many different fluorescences on individual cells has two requirements: multiple non-colinear excitation beams and a spectral resolution which minimizes emission overlap. We minimized detector cross-talk by appropriate selection of dyes and excitation conditions (including laser wavelength and power). In addition, we selected optimal optical filters to minimize signal overlap without losing too much intensity (Fig. 2).

Fluorochromes chosen for immunophenotyping should be as ''bright'' as possible in order to achieve the greatest sensitivity. Brightness, as used in this report, is an empirical quantity that relates not only physical properties, including the extinction coefficient, lifetime, and quantum efficiency of a given fluor, but also detector sensitivity, background noise, and autofluorescence contributions from cellular material in that portion of the spectrum. To date, fluorescein (FITC), Texas Red (TR), the phycobiliproteins phycoerythrin (PE) and allophycocyanin (APC), and a resonance energy transfer tandem dye Cy5PE have been commonly used in flow cytometry analyses because they are bright and spectrally well-resolved dyes. To extend the capabilities to 8 color analyses, we chose the new tandems Cy7PE and Cy7APC (23), because these are well resolved spectrally from the others. In addition, we use Cascade Blue (CB) excited by a 407 nm Krypton laser line (manuscript in preparation).

The fluorescence spectra of these eight dyes are shown in Figure 3. For any given excitation beam, the fluorescence emissions are well resolved, such that interference filters that selectively pass the primary fluorescence of interest can be easily chosen.

Useful Brightness of Fluorochromes

In order to assess the brightness (and utility) of these fluorochromes, direct conjugates of anti-human CD8 were conjugated with each. Saturating concentrations of the antibodies were used to stain human PBMC in combination with either FITC CD3 or CB CD3; the histograms corresponding to the $CD3^+$ cells from each of the stained samples are shown in Figure 4. Each of the fluorescent dyes resolves CD8 T cells from other T cells very well; all of the dyes except CB appear to separate these cells from $CD8^-$ T cells as well or better than FITC. Indeed, quantification of the peak positions shows that this is the case, as shown in Table 1.

The useful brightness of a conjugate can be evaluated in several ways. The simplest is the ratio of the median signals of the positive to unstained cells. However, this does not take into account that the distribution of the negative population may be quite different for different spectral regions. Indeed, for the far-red channels there are so few photoelectrons (on the order of 1–10) collected for unstained cells that the absolute signal level of these cells is not necessarily meaningful.

Another measure of useful brightness is the resolution of the two peaks (positive and negative). In Table 1, this value was calculated by normalizing the signal level of the positively stained cells to a measure of the variation in the negative population. This is a value akin to a ''t-score''; it is related to how well separated the peaks actually are and makes no assumptions about absolute signal levels for either the stained or unstained populations. For our instrument, the amount of signal in the far-red channels is so low for the APC and Cy7APC channels that the ''autofluorescence'' peak actually bifurcates—into events with zero or one photoelectrons. This increases the peak width of the autofluorescent cells, thereby significantly reducing this particular brightness estimator for APC and Cy7APC.

A final measure of brightness also takes into account the general ''stickiness'' of the reagents—the tendency of some fluorochrome conjugates to display increased nonspecific binding to cells (Table 1). To quantify this value, the signal level of the positively stained cells is compared to the signal level of $CD8^-$ cells present in the stained population—cells that have autofluorescence equivalent to the $CD8^+$ lymphocytes (data not shown).

All three measures of brightness give the same general order when comparing reagents (the main difference being the absolute value of the computed brightness). CB is the least bright, being about one-third the brightness of FITC. FITC, Cy7PE, and Cy7APC are roughly equivalent. TR is about threefold brighter than FITC (but suffers from unusually high background binding commonly observed for TR reagents). Finally, PE, Cy5PE, and APC are 5–10 times as bright as FITC. This order is consistent with the

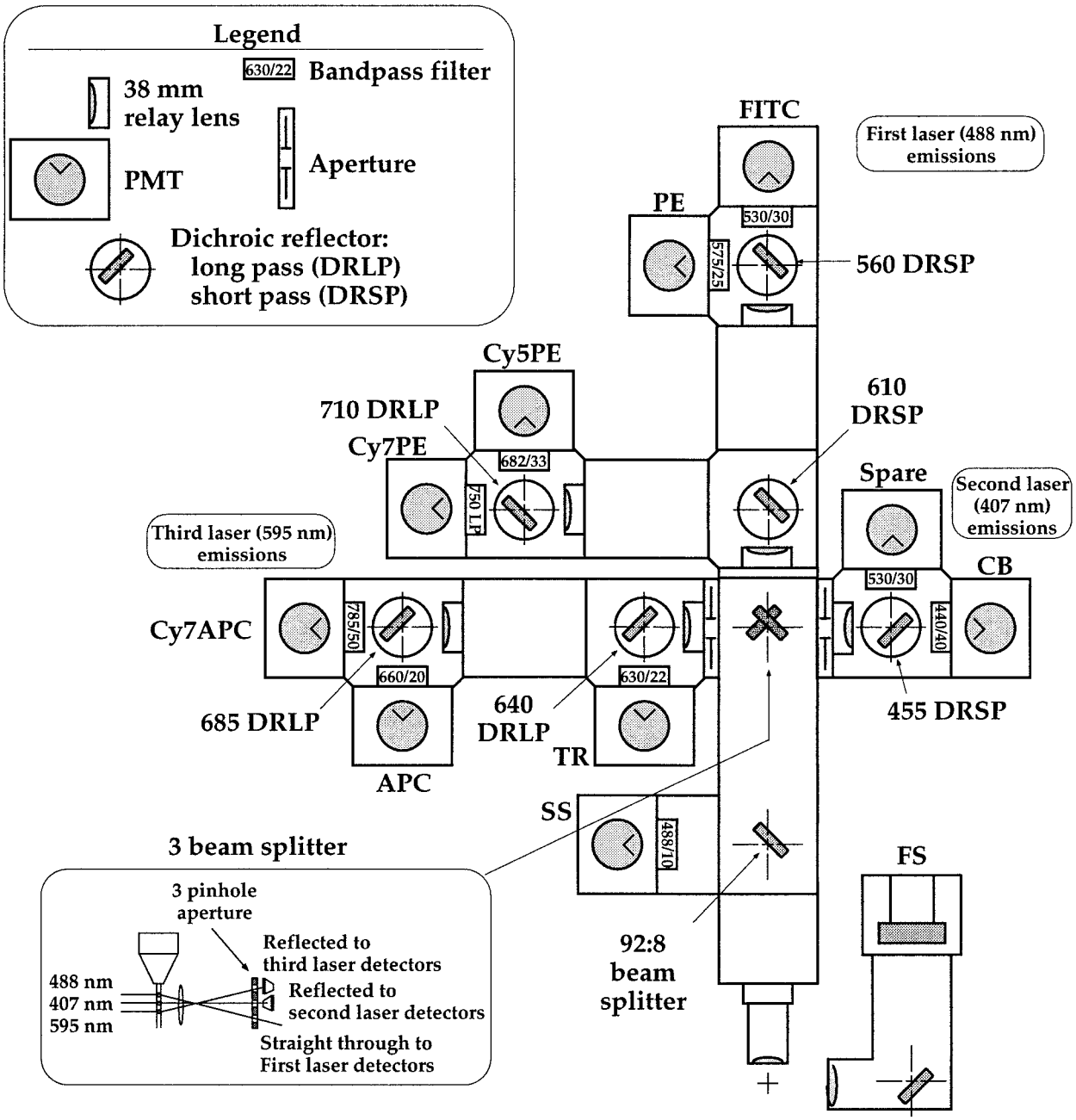

FIG. 2. Diagrammatic layout of the optics. The block diagram shows the layout of the 11 detectors on the modified FACStarPlus bench. For this report, the ''UV2'' detector was not used. The Cy5PE and Cy7PE detectors are rotated 90 degrees out of the plane of the optics block in order to accommodate the orientation of the beam splitter (all splitter blocks have ''left-hand'' turns only). Thus, the cable connections for these two PMTs point away (backwards) from the nozzle area, whereas all other PMT connections point up. Note the presence of additional relay lenses in the extended fluorescence pathways in order to refocus the emission on the detectors. The side scatter beam splitter is achromatic, and reflects 8% of incident light. The ''three-beam'' splitter has two mirrors mounted at right angles to deflect the second and third laser emissions; the first laser emission passes underneath the mirrors.

brightest reagents being farther red in the spectrum; however, for the Cy7 tandems the transfer efficiency as well as the detector efficiency at >750 nm is dropping off sufficiently that their brightness is less than APC or Cy5PE.

Complex Compensation

While the fluorescence emissions are well-resolved, there is still considerable spectral overlap. In other words, most of the fluorochromes show appreciable signal in more than one detector. The exception to this is CB, which has no emission components from the detectors for 488 nm or 595 nm excited dyes; likewise, none of the other fluors is excited by the 407 nm line to emit at 440 nm.

To correct for the spectral overlap, compensation must be performed to make the measured values orthogonal.

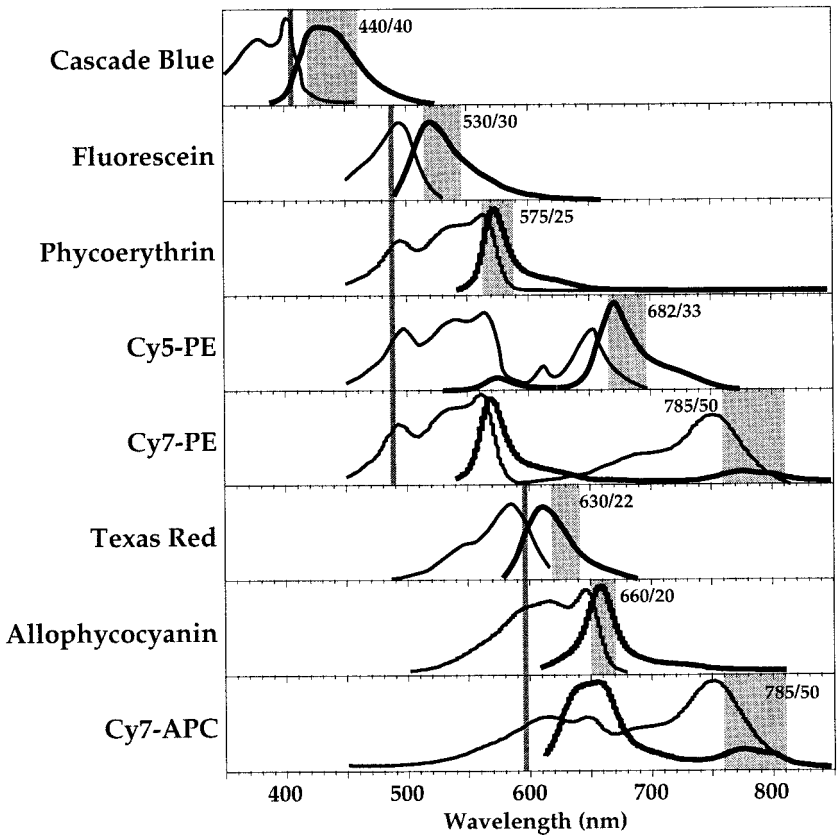

FIG. 3. Fluorescence spectra of the eight fluorochromes used in these studies. Excitation and emission spectra for the fluorochromes are uncorrected for detector sensitivity. Thus, the relatively low peak in the far-red region for the Cy7 emissions is not necessarily reflective of the brightness of Cy7 reagents. In addition, the extremely low autofluorescence of cells in the far red increases the signal-to-noise for these reagents. The wavelengths of the excitation beams are shown by vertical bars; the bandpass region for each detector is shown as a shaded region.

Because of the great number of different corrections required for the 8 color system, compensation cannot be performed manually using pair-wise controls, as are found on commercial flow cytometers; complete compensation requires computer assistance. Because we currently do not have such a system designed into the electronics, we collect uncompensated signal values and use software to compensate the data at the time of analysis (24).

To compensate a sample properly, we singly stain cells with representative reagents for each fluorochrome. These singly stained samples are collected and analyzed; the compensation matrix can be computed from the resulting fluorescence measured in all of the channels. A typical spillover (spectral overlap) matrix is given in Table 2. The values in this table directly show the amount of fluorescence from any given fluorochrome detected in the other channels.

In order to perform the compensation, this matrix must be inverted to generate the compensation coefficient matrix (24). The matrix resulting from this operation in Table 2 is shown in Table 3; the values in Table 3 are those that correspond most closely to the compensation values that are set on typical instruments performing pair-wise compensation between two fluorescence channels.

Application to Murine Leukocyte Staining

We explored the utility of using eight colors for flow cytometric phenotyping of mouse bone marrow cells. In this case, in place of FITC-conjugated monoclonal antibodies we used the FITC detector to detect BEX GFP (blue-excited Green Fluorescent Protein) expression (2). Unlike other GFPs which lack the S65T mutation, BEX is primarily excited at 488 nm, with little excitation at 407 nm. Thus, the krypton laser can be used for the excitation of CB without significant compensation with BEX (manuscript in preparation). The mice from which we obtained bone marrow expresses BEX as a transgene driven by an H2-K (class I MHC) promoter; expression of the BEX GFP is closely correlated with H2-K expression in individual cells (manuscript in preparation). The transgenic mice used in these experiments have detectable BEX expression in 20–40% of hematopoietic cells. As transgenic mice derived from a separate founder exhibit GFP transgene expression in almost all bone marrow cells (RG, unpublished results), the lower frequency of BEX expression in these animals is most likely due to a position effect at the transgene insertion site.

In order to investigate transgene expression within the B cell lineage, we stained cells with the panel of seven monoclonals indicated in Figure 5 (IgM, CD22, IgD, B220, Gr-1, AA4.1, and HSA). In addition, the dye propidium iodide was used to detect and exclude dead cells (6) in the Cy5PE channel, without significant overlap with B220-Cy5PE-positive cells. Figure 5 shows that a significant fraction of Gr-1$^+$ cells (a marker of the myeloid/granulocyte lineage (8)) express GFP. Smaller fractions of B220-

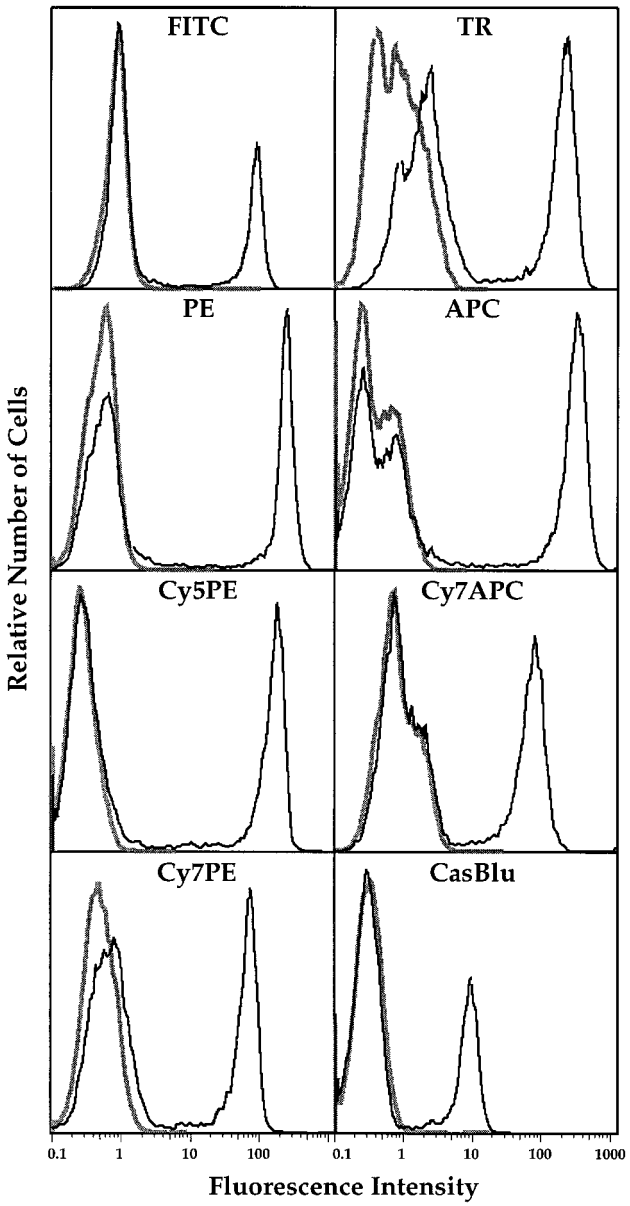

FIG. 4. Comparison of the staining properties of anti-CD8 conjugated to each of the eight fluorochromes. Anti-CD8 was conjugated to each of the fluorochromes; the reagent was used in saturating titers to stain human peripheral blood mononuclear cells. In addition, CD3 was used as a counterstain in each sample; for CB CD8, FITC CD3 was used; for all others, CB CD3 was used. Histograms of unstained lymphocytes and the stained $CD3^+$ T cells are overlaid for each detector. The relative brightness of each of these reagents, computed in various ways, is shown in Table 1.

Table 1
Relative Brightness of the Eight Probes in Immunofluorescence Staining

Fluor	%CD8+[1]	Relative brightness,[2] with respect to: AF[3]	Background[4]	AF width[5]
CB	36.0	0.3	0.3	0.2
FITC	37.1	1.0	1.0	1.0
PE	37.0	4.6	4.5	3.0
Cy5PE	36.3	6.2	6.2	4.3
Cy7PE	36.0	1.4	1.1	0.8
TR	38.1	2.8	1.2	0.8
APC	36.5	9.2	8.7	2.2
Cy7APC	35.2	0.9	0.9	0.4

[1]Cells were stained with saturating concentrations of CD8 conjugated to the listed fluorescent probes. The value is the percent of lymphocytes staining brightly for CD8 (CD8 T cells).

[2]Brightness values are normalized separately for each column, such that FITC = 1.0.

[3]Median fluorescence of CD8+ cells divided by the median of unstained lymphocytes (i.e., autofluorescence, or AF).

[4]Median fluorescence of CD8+ cells divided by the median of CD8− lymphocytes in the same tube (NK cells, dimly staining for CD8, were excluded).

[5]Median fluorescence of CD8+ cells divided by twice the difference of the 67th and 50th percentiles of the unstained population (i.e., normalizing by the approximate standard deviation of the autofluorescence of unstained cells).

positive cells (a B lineage marker in most cases (3, 25)) and Gr-1-negative, B220-negative cells express BEX. $Gr\text{-}1^+$ cells were excluded from further analyses; this gating eliminates not only $Gr\text{-}1^+$ cells but also the most autofluorescent cells as well as cells that express Fc receptors. Examination of all $B220^+$ Gr-1-negative cells for the expression of IgD and IgM (data not shown) revealed three distinct populations of cells. For convenience, we define IgD^+ $IgM^{lo/+}$ cells as Population I, IgM^+ $IgD^{-/lo}$ (i.e., IgM^+, IgD non- or low-expressing cells) as Population II, and IgD^- IgM^- as Population III. Pop. I cells, expected to be composed predominantly of mature, recirculating B cells (1, 9) have the largest percent of GFP-positive cells. Pop. II, with fewer GFP^+ cells, contains immature IgM^+ cells (10). Pop. III, which includes mostly pro- and pre-B cells, has the least proportion of GFP^+ cells.

These $B220^+$ $Gr\text{-}1^-$ populations can be defined more specifically using the monoclonal AA4.1 (Fig. 5). AA4.1 has been used previously to isolate stem cells (11), B cell precursors (5, 14-17), and ''bi-potent'' progenitors that can differentiate along myeloid or B cell pathways (4, 12). It has also been noted that approximately 50% of cells with surface Ig in bone marrow were $AA4.1^+$ (15). Using a bright APC conjugate of AA4.1, it is evident that most B220-positive bone marrow cells express AA4.1. Figure 5 further shows that Populations I, II, and III are differentially represented among $AA4.1^+$ and $AA4.1^-$ cells; most notably, Pop. I is significantly underrepresented in $AA4.1^+$ cells. Finally, for each of the fine subsets plots of CD22 expression (a mature B cell marker) versus GFP expression and CD22 versus HSA expression (mature B cells are HSA intermediate, low, or null) are shown.

In $AA4.1^+$ cells, Pop. I is comprised mostly of $CD22^+$ HSA^{lo} cells (in agreement with (7)). Pop. II is uniformly $CD22^{-/lo}$ and HSA^+. Pop. III, which includes mostly pro- and pre-B cells is $CD22^{-/lo}$ and is mostly HSA^+ (Fr. B,C,D using Hardy's criteria (10)). Pop. III includes some $HSA^{-/lo}$ cells (predominantly Fr. A (10, 14)).

In contrast, $AA4.1^-$ cells have a striking increase in the fraction of IgD^+ cells. Note that Pop. II is reduced among

Table 2
Spillover Matrix for 8 Color Flow Cytometry[a]

	Emission detector						
	First laser (488 nm)				Second laser (595 nm)		
Fluor	FITC	PE	Cy5PE	Cy7PE	TR	APC	Cy7APC
FITC	100	20	1.6	0.26	0.00	0.00	0.24
PE	1.6	100	8.8	1.1	0.60	0.02	0.28
Cy5PE	0.59	8.4	100	16	0.61	5.3	7.8
Cy7PE	1.4	25	3.8	100	0.22	0.03	12
TR	0.08	0.13	1.3	0.19	100	6.1	6.6
APC	0.11	0.06	6.6	1.1	28	100	76
Cy7APC	0.20	0.10	0.33	1.6	2.9	3.5	100

[a]Cascade Blue is not in the table since there is no spillover between its detector and any other detector. Each value is the percentage of a fluor's signal measured in each of the seven detectors (normalized to 100% for the fluor's cognate detector). Thus, each row is related to the emission spectrum of the fluor named in the first column—given the particular combination of lasers, filters, detectors, and PMT voltages used in our instrument. For instance, the measured signal voltage of FITC in the PE channel is 20.2% of that in the FITC channel. Since FITC is not excited by the dye laser, there is essentially no contribution of FITC fluorescence into the second laser channels. The top left and bottom right quadrants of the matrix represent intra-laser spillovers; the other two quadrants are inter-laser spillovers.

Table 3
Compensation Matrix for 8 Color Flow Cytometry[a]

	Emission channel						
	First laser (488 nm)				Second laser (595 nm)		
Fluor	FITC	PE	Cy5PE	Cy7PE	TR	APC	Cy7APC
FITC		20	−0.14	0.07	−0.13	0.00	0.19
PE	1.6		8.8	−0.39	0.69	−0.49	−0.03
Cy5PE	0.28	4.2		16	−1.0	5.3	1.8
Cy7PE	0.97	25	1.6		−0.16	−0.47	12
TR	0.06	0.05	0.85	−0.05		6.0	2.0
APC	−0.08	−0.25	6.1	−1.2	26		74
Cy7APC	0.18	−0.35	0.05	1.6	2.0	3.4	

[a]Each value represents the compensation percentage value that needs to be applied to the original signals in order to achieve orthogonality. These values are equivalent to the compensation that would be selected on an instrument capable of performing the pairwise compensations on all parameters (i.e., the FITC − %PE compensation value is 20.%). Those values greater (in absolute magnitude) than 0.4% can be considered significant compensations; all others are shaded. These values were obtained by inverting, normalizing, and negating the spillover coefficient matrix in Table 2; the diagonal elements were removed for clarity.

$AA4.1^-$ cells and the distribution of IgM of this population is quite different from that of $AA4.1^+$ cells. For example, in the $AA4.1^-$ compartment, Pop. III includes significantly more $CD22^+$, GFP^+, and HSA^- cells than are found among $AA4.1^+$ Pop. III cells. $AA4.1^+B220^+$ IgM^-IgD^- cells are almost exclusively pro- and pre-B cells (data not shown). The corresponding $AA4.1^-B220^+IgM^-IgD^-$ population may contain mature B cells, as suggested by the presence of $CD22^+$ GFP^+ HSA^- cells. We have yet to examine these cells for surface IgG. It will be interesting to determine if memory or antibody secreting cells reside within this population.

Application to Human Leukocyte Staining

Peripheral T cells in the human can be divided into a number of subsets. These divisions can be classified as lineages (e.g., CD4 versus CD8 T cells) and as differentiation stages (e.g., naive versus memory). Based on functional and phenotypic studies, naive T cells have been defined as those T cells expressing CD45RA and CD62L (19, 20, 22); memory cells lack one or both of these markers. We explored the phenotypic heterogeneity of naive and memory T cells within several T cell lineages in human peripheral blood.

To divide the T cells into lineages, we used antibodies to CD3 (to define T cells), CD4, CD8, and the γδ-T cell receptor. To define differentiation stages, we used antibodies to CD45RA and CD62L. Finally, to explore the heterogeneity of these subsets we examined the expression of CD11a and CD57.

Figure 6 shows the progressive gating to define six T cell lineages. We can identify two lineages of γδ T cells ($CD4^+$ and $CD4^-$; the latter express zero to low levels of CD8). Of the αβ T cells, we identify four distinct lineages: the CD4 helper cells ($CD4^+CD8^-$), the CD8 cytotoxic/suppressor cells ($CD4^-CD8^+$), the double-negative cells (DN, $CD4^-CD8^-$), and cells which express CD4 and dimly express CD8 ($CD8^{dim}$). The $CD8^{dim}$ T cells are phenotypically and functionally distinct from the other subsets (27);

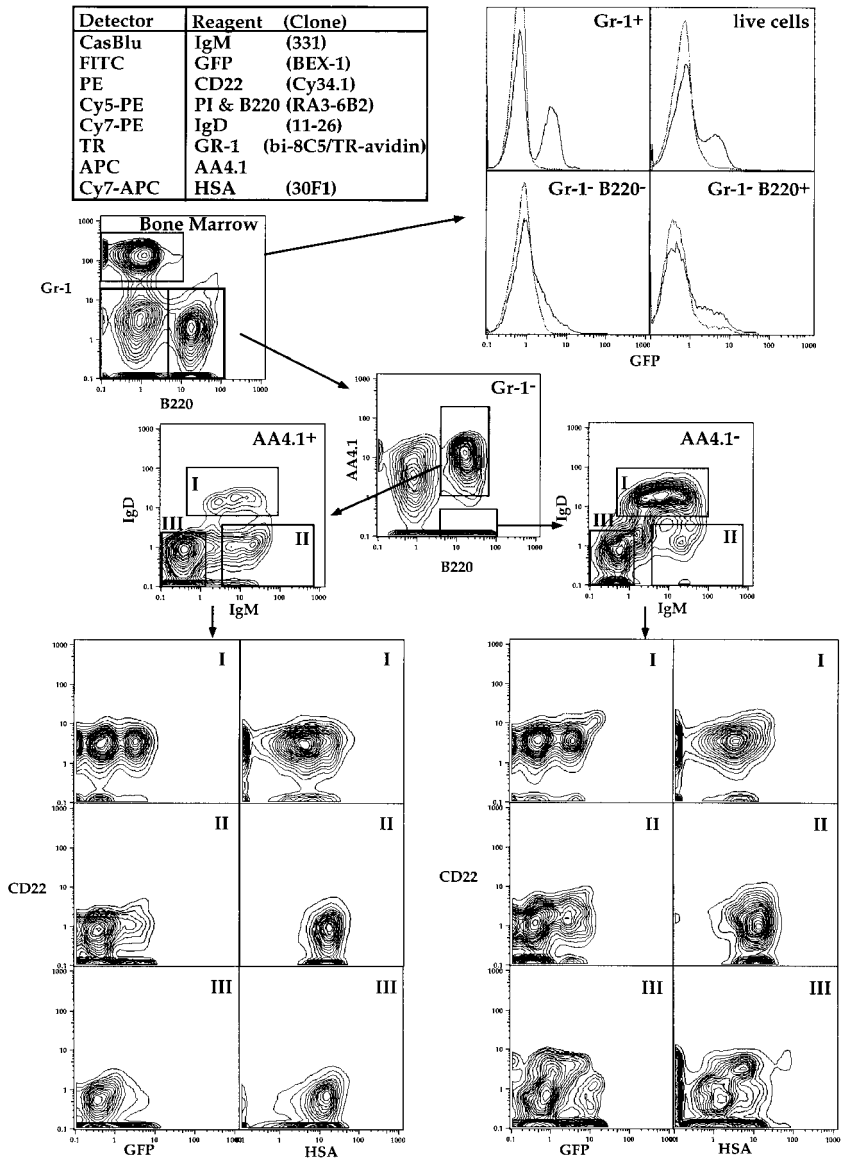

FIG. 5. 8 color flow cytometric analysis of murine bone marrow cells. These plots are all derived from the same single-tube collection of 1×10^5 cells. Bone marrow cells were isolated from a 3-month-old mouse transgenic for BEX-1 GFP driven by a H-2K (murine Class I MHC) promoter. Similar results (except for GFP expression) were obtained with nontransgenic mice of comparable genetic background (data not shown). Ungated data were collected for 100,000 cells. In order to establish a compensation matrix, data were also recorded from separate samples of cells that were singly stained with bright reagents. For compensation of the GFP signal, transgenic spleen cells were analyzed and used in the compensation matrix in the "FITC" channel. Dead cells (defined as propidium iodide-bright cells in the Cy5-PE channel) were excluded from post hoc analyses (8% of cells). All two-dimensional plots are 5% probability contour plots. Boxes indicate software gates drawn for analysis of data. The combination of reagents used to stain bone marrow cells simultaneously and the detector used for each reagent is indicated in the box. The upper left panel depicts Gr-1 (8C5) (a marker of the myeloid/granulocyte lineage) expression versus B220 (expressed predominantly by B lineage cells). In the top right, histograms showing GFP expression in all live cells, $8C5^+$, $8C5^-B220^-$, and $8C5^-B220^+$ cells are shown. The lighter histogram indicates fluorescence from nontransgenic mouse bone marrow using equivalent staining and gating. The center panel shows the expression of AA4.1 and B220 on Gr-1^- cells. These cells are divided into AA4.1+ or AA4.1− cells; the expression of IgD and IgM is then used to further subdivide these cells into three classes each (population I, IgD^+, $IgM^{lo/+}$; II, IgD^-IgM^+; and III, IgD^-IgM^-). Data from each of these 12 populations is displayed in the panels, as CD22 (a marker of mature B cells) vs. GFP expression, and CD22 vs. HSA expression are shown. HSA is expressed on immature and germinal center B cells. (See text for a description of the subsets.)

in particular, they express the CD8αα homodimer rather than the CD8αβ heterodimer. Finally, within the αβ T cells we can identify, in general, at least four subsets based on the differentiation markers CD45RA and CD62L (Fig. 6).

CD57 and CD11a have been used previously to distinguish differentiated subsets of T cells. CD11a is expressed on all T cells, but occurs at higher levels on memory subsets (26). The expression of CD57 is reciprocal to CD28; its expression has been thought to mark terminally differentiated T cells (13).

Examination of the T cell subsets for CD57 and CD11a reveals several features that are consistent across all lineages. First, naive T cells, as expected, express lower levels of CD11a and essentially no CD57. Memory T cells that express CD62L (and are $CD45RA^-$) can be divided into cells which express low or high levels of CD11a—although this distinction is often lost in the smear of the distribution. In addition, there is a subset which dimly expresses CD57 (and, perhaps surprisingly, relatively low CD11a). The $CD45RA^-CD62L^-$ subset has a greater frequency of cells which express CD57; the highest frequency of CD57 expression (and brightest expression) is found on the $CD45RA^+$ $CD62L^-$ subset. It is remarkable that lineages which are functionally so distinct as CD4 and CD8 T cells have differentiation stages with such highly conserved phenotypic properties.

DISCUSSION

We report here some of the first experiments performed using 8 color, 10-parameter flow cytometry analysis. While at first this technology may seem esoteric, it has become apparent that this degree of resolution is necessary for identifying unique cell populations within the immune system. Based on functional studies, we believe that, using

8 color phenotyping, we are beginning to identify phenotypically and functionally homogeneous subsets—a primary goal of flow cytometric analysis.

The power of the 8 color analysis is readily apparent by the complex data presented in Figures 5 and 6. These two figures represent analysis of a single tube (each); data for $1–3 \times 10^5$ cells was collected. From this data, we are able to resolve dozens of phenotypically distinct T cell subsets in human peripheral blood.

In addition to the ability to finely subset lymphocytes, the 8 color technology gives us the ability to combine phenotypic and functional analysis to a degree previously unattainable. For instance, we can subset T cells using five different antibodies (CD3, CD4, CD8, CD45RA, and CD62L), and then use two antibodies to measure cytokine profile (e.g., IL4 and γ-IFN) and one color to measure apoptosis (annexin V). Thus, we can quantify several functional capacities of fine T cell subsets. This will be crucial to understanding whether phenotypic heterogeneities such as that seen in Figure 6 are meaningful or not.

The murine staining example demonstrates the power of 8 color flow cytometry analysis for immunophenotyping as well as detection of a GFP reporter gene. Based on this figure alone, we can divide murine bone marrow B lineage cells into at least six subsets. In addition, we show that several of these subsets display further heterogeneity and exhibit unique features compared to other populations. Our general strategy is to select reagents such that the gating uses both exclusion and inclusion criteria, i.e., Gr-1 expression as an exclusion criterion and B220 expression as an inclusion criterion. The lineage-defined cells are then examined for markers of interest, e.g., AA4.1—for which there is little information about expression during differentiation. Correlating expression of this marker with other well-defined cell surface proteins (e.g., IgM, IgD, CD22, HSA), as well as a BEX reporter of the H2K promoter, can be used to make inferences about B cell maturation in bone marrow. Finally, we demonstrated that BEX transgenic mice can be evaluated for GFP expression simultaneously with the expression of seven distinct cell surface antigens. This lays the foundation for exploiting the power of 8 color flow cytometry for evaluation of GFP reporter genes within defined immune system subsets.

There were a number of obstacles to achieving 8 color analysis. First was the development of appropriate reagents (some of which are described in detail elsewhere (2, 23)). Antibodies conjugated to most of these reagents are commercially available; at this time, the Cy7 tandem and CB conjugates must be synthesized in the laboratory (21).

The second obstacle was the electronics. Currently, only the Cytomation MoFlo electronics module is able to collect ten measurable parameters and use three different delay timers (for three-laser excitation); thus, we built a hybrid instrument using these electronics. The extended optical layout has been somewhat problematic; the emission paths are very long and it is critical to maintain proper beam path alignment at every juncture.

Finally, we found it necessary to develop an entirely new software package capable of performing the multidimensional compensation (24), plus organizing and presenting the complex datasets that arise from multiparameter analyses.

Compensation has become one of the most critical aspects of the analysis. Whereas in 2 color staining compensation is easy to assess at the time of collection, the multiple interactions make it impossible to do so with 8 color staining. In addition, it is important to remember that each lot of a tandem dye (Cy5PE, Cy7PE, Cy7APC) will have different spectral characteristics—as will APC reagents obtained from different manufacturers. In general, compensation will be different for two different Cy5PE reagents. We collect data for a single-stained sample for each different lot of each of the tandems used in an experiment. In a typical four-tube experiment (using as many as 32 different reagents), we would have approximately a dozen different compensation samples. The software selectively applies the appropriate compensation matrices to each of these analyses.

It is important to note that many of the values in a typical compensation matrix (such as shown in Table 3) are negative. This is because of the interaction between different compensation values. For instance, FITC has a significant contribution of fluorescence to the Cy5PE channel. A pair-wise compensation between FITC and CY5PE would require about 1.6% compensation. However, the PE to Cy5PE compensation already removes a contribution of the FITC (because of the contribution of FITC into the PE channel). Indeed, this second compensation removes too much of the FITC signal (because the spectral overlap of PE into the Cy5PE channel compared to the PE channel is more than that of the FITC into the Cy5PE channel compared to FITC in the PE channel). The net result is that some of the FITC signal must actually be added back into the Cy5PE channel—i.e., a negative compensation value. In addition to the sheer number of compensations required, the interaction between the values makes it essentially impossible to set the compensation values manually.

An unfortunate disadvantage to the large number of compensations is the concomitant loss in dynamic range. Part of this loss results from often having to subtract several significant signal components from other dyes before evaluating the residual signal due to the dye of

FIG. 6. An example of 8-color staining of human lymphocytes. These plots are all derived from the same single-tube collection of 3×10^5 cells. Peripheral blood mononuclear cells were stained with FITC CD11a, PE TcR γδ, Cy5PE CD45RA, Cy7PE CD62L, TR CD4, APC CD57, Cy7APC CD8, and CB CD3. Progressive gating is shown for lymphocytes (top left, based on forward and side scatter), and αβ or γδ T cells. The γδ T cells are further divided based on expression of CD4. The αβ T cells are divided on the basis of CD4 and CD8 expression into four lineages. Each of the lineages is further subdivided into differentiation stages based on CD45RA and CD62L expression. Finally, the expression of CD11a and CD57 is compared for the two γδ lineages, and the four subsets of each of the four αβ lineages. On these plots, boxes and lines are positioned identically within each lineage to allow for comparison of the relative expression of these markers. All two-dimensional graphs are 5% probability contour plots; some have outlier events marked.

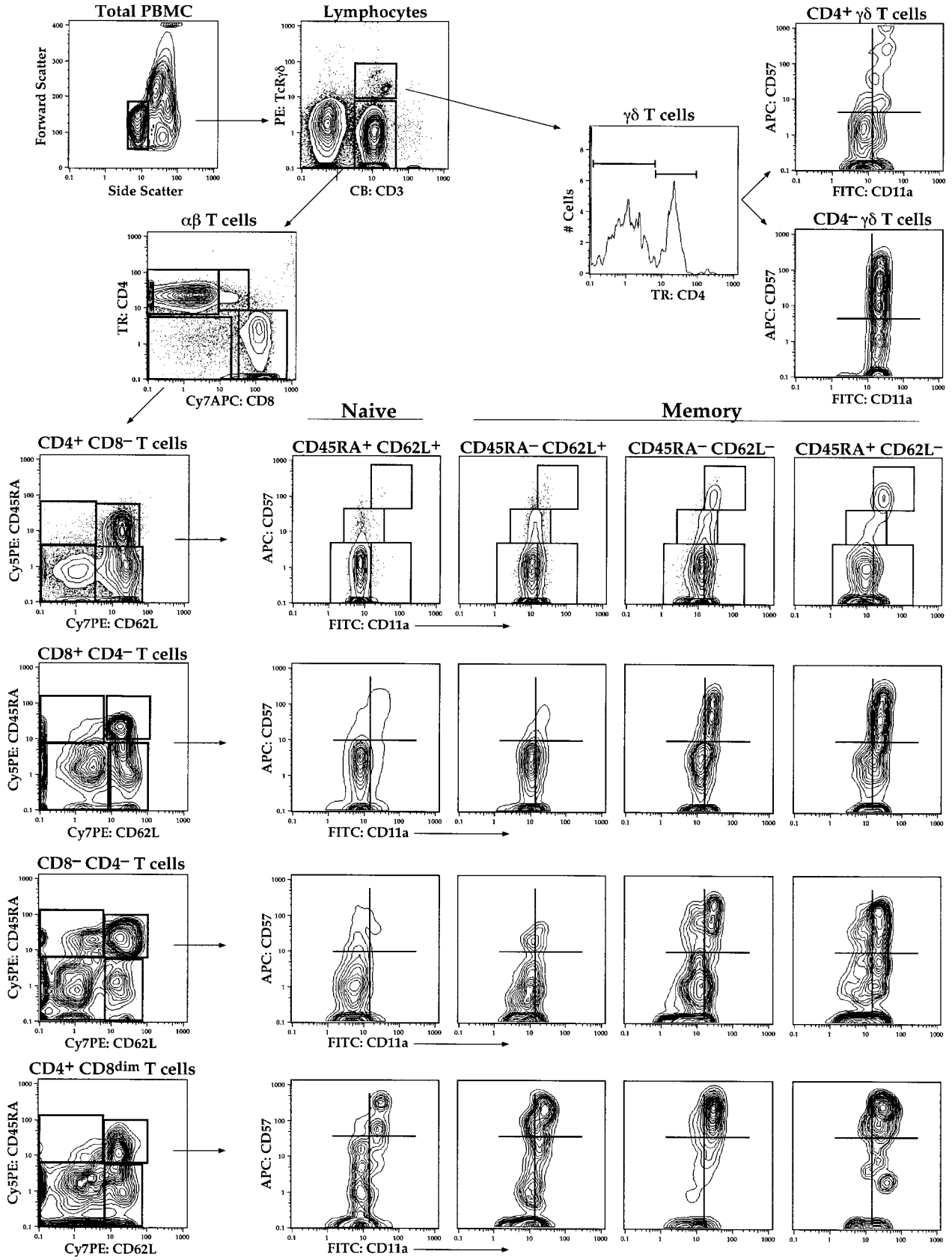

Roederer et al., Figure 6

FIG. 6.

interest on that measurement channel. Additional losses are introduced into the compensation calculations because of imperfect logarithmic conversion of the signals. Our logarithmic amplifiers show as great as 5% deviation across the four-decade range of signals. The deviation leads to inaccuracies in computing the absolute signal intensity from the digitized log data. The absolute signal intensity is required for the linear transformation used in compensation; for some channels, this error is introduced several times as multiple parameters have significant compensations into that channel. The net result is a broadening of all distributions (and especially the ''negative'' populations with the lowest signal levels); a broader distribution means less resolution of positive and negative populations and is mathematically equivalent to a loss in dynamic range.

Future instrumentation developments should focus on performing the compensation ''live''—i.e., before conversion to log data. Alternatively, collection of very high resolution linear values (at least 16 bit data) allows for accurate compensation during the analysis stage (software logarithmic conversion would then be used to present the data in the desired format).

Perhaps one of the most important lessons that we have learned in the application of 8 color flow cytometry is that there is a great need for new software analysis tools. Some of these tools, such as compensation and log-conversion of linear data, are currently available in only a few software packages. More importantly, however, is the requirement for software which allows for logical analysis of the highly complex datasets generated by >5 parameter collections. New paradigms for the analysis as well as presentation of data are needed. For example, in both Figures 5 and 6 there is much more complexity within the datasets than we are able to show here—indeed, it is nearly impossible to present raw data from these analyses in a way which can be quickly grasped by even experienced persons.

Our 8 color studies have demonstrated that this technology is not only powerful, it has quickly become requisite for understanding the complexity of the immune system. Before this technology can be used by a wide variety of researchers, however, there are still several obstacles that must be overcome: Manufacturers must start making instrument benches that can be extended to more than seven or eight parameters. These instruments need to have computer-assisted instrument set-up, calibration, and data collection. Software developers have to give us new and powerful tools, and the reagent manufacturers have to start supplying many more fluorochrome-conjugated versions of their monoclonal antibodies.

What is the future for increasing the number of colors? At this time, there is only a single color from the Krypton 407 nm laser line; there are additional fluorochromes which can be excited efficiently by this laser line and have emissions that are spectrally resolved from CB (manuscript in preparation). In addition, there is a mutant of GFP, VEX, which is efficiently detected using this system (2). These have already provided us with a ninth color; it is certainly conceivable that there are tandem dyes that can be specifically excited at 407 nm and emit in the orange or red region of the spectrum that will provide even more independent colors. It may also be possible to squeeze more colors out of the 488 nm line—for example, by using Cy5.5-PE tandems—however, there is already so much spectral overlap that these may be of little value. The increases in colors will more likely come from the use of additional excitation beams in the far red, using infra-red fluorescent dyes. In any case, it is clear that we have not yet reached the limit on the number of available colors and will, over the next decade, probably achieve nearly a dozen useful fluorescence parameters.

ACKNOWLEDGMENTS

We thank Becton Dickinson for the generous donation of the FACStarPlus optical bench. We are grateful to Drs. Chris Klug and Irving Weissman for collaborating with us on analysis of their GFP transgenic mouse. We thank Gina Jager for excellent technical assistance, Ometa Herman for animal husbandry and technical support, Dr. Nicole Baumgarth and other members of the Herzenberg laboratory for helpful advice, and Drs. Aaron Kantor and Masahiko Amano for the preparation of some murine reagents and helpful advice.

LITERATURE CITED

1. Allman DM, Ferguson SE, Lentz VM, Cancro MP: Peripheral B cell maturation. II. Heat-stable antigen(hi) splenic B cells are an immature developmental intermediate in the production of long-lived marrow-derived B cells. J Immunol 151:4431–4444, 1993.
2. Anderson MT, Tjioe IM, Lorincz MC, Parks DR, Herzenberg LA, Nolan GP, Herzenberg LA: Simultaneous fluorescence-activated cell sorter analysis of two distinct transcriptional elements within a single cell using engineered green fluorescent proteins. Proc Natl Acad Sci USA 93:8508–8511, 1996.
3. Coffman RL: Surface antigen expression and immunoglobulin gene rearrangement during mouse pre-B cell development. Immunol Rev 69:5–23, 1982.
4. Cumano A, Paige CJ: Enrichment and characterization of uncommitted B-cell precursors from fetal liver at day 12 of gestation. Embo J 11:593–601, 1992.
5. Cumano A, Paige CJ, Iscove NN, Brady G: Bipotential precursors of B cells and macrophages in murine fetal liver. Nature 356:612–615, 1992.
6. Dangl JL, Parks DR, Oi VT, Herzenberg LA: Rapid isolation of cloned isotype switch variants using fluorescence activated cell sorting. Cytometry 2:395–401, 1982.
7. Erickson LD, Tygrett LT, Bhatia SK, Grabstein KH, Waldschmidt TJ: Differential expression of CD22 (Lyb8) on murine B cells. Int Immunol 8:1121–1129, 1996.
8. Fleming TJ, Fleming ML, Malek TR: Selective expression of Ly-6G on myeloid lineage cells in mouse bone marrow. RB6-8C5 mAb to granulocyte-differentiation antigen (Gr-1) detects members of the Ly-6 family. J Immunol 151:2399–2408, 1993.
9. Forster I, Vieira P, Rajewsky K: Flow cytometric analysis of cell proliferation dynamics in the B cell compartment of the mouse. Int Immunol 1:321–331, 1989.
10. Hardy RR, Carmack CE, Shinton SA, Kemp JD, Hayakawa K: Resolution and characterization of pro-B and pre-pro-B cell stages in normal mouse bone marrow. J Exp Med 173:1213–1225, 1991.
11. Jordan CT, McKearn JP, Lemischka IR: Cellular and developmental properties of fetal hematopoietic stem cells. Cell 61:953–963, 1990.
12. Kee BL, Paige CJ: In vitro tracking of IL-7 responsiveness and gene expression during commitment of bipotent B-cell/macrophage progenitors. Curr Biol 6:1159–1169, 1996.
13. Kern F, Ode-Hakim S, Vogt K, Hoflich C, Reinke P, Volk HD: The enigma of CD57+CD28− T cell expansion—anergy or activation? Clin Exp Immunol 104:180–184, 1996.
14. Li YS, Wasserman R, Hayakawa K, Hardy RR: Identification of the earliest B lineage stage in mouse bone marrow. Immunity 5:527–535, 1996.
15. McKearn JP, Baum C, Davie JM: Cell surface antigens expressed by subsets of pre-B cells and B cells. J Immunol 132:332–339, 1984.

16. McKearn JP, McCubrey J, Fagg B: Enrichment of hematopoietic precursor cells and cloning of multipotential B-lymphocyte precursors. Proc Natl Acad Sci USA 82:7414–7418, 1985.
17. McKearn JP, Rosenberg N: Mapping cell surface antigens on mouse pre-B cell lines. Eur J Immunol 15:295–298, 1985.
18. Moore WA, Kautz RA: Data analysis in flow cytometry. In: Handbook of Experimental Immunology, 4th ed., Weir DM, Herzenberg LA, Blackwell CM, Herzenberg LA (eds). Blackwell Scientific Publications, Edinburgh, 1986, 30.1–30.11.
19. Picker L, Treer J, Ferguson D, Collins P, Buck D, Terstappen L: Control of lymphocyte recirculation in man. I. Differential regulation of the peripheral lymph node homing receptor L-selectin on T cells during the virgin to memory cell transition. J Immunol 150:1105–1121, 1993.
20. Rabin RL, Roederer M, Maldonado Y, Petru A, Herzenberg LA, Herzenberg LA: Altered representation of naive and memory CD8 T cell subsets in HIV-infected children. J Clin Invest 95:2054–2060, 1995.
21. Roederer M: Conjugation of monoclonal antibodies. http://cmgm.stanford.edu/~roederer/abcon/ (1996).
22. Roederer M, Bigos M, Nozaki T, Stovel RT, Parks DR, Herzenberg LA: Heterogeneous calcium flux in peripheral T cell subsets revealed by five-color flow cytometry using log-ratio circuitry. Cytometry 21:187–196, 1995.
23. Roederer M, Kantor AB, Parks DR, Herzenberg LA: Cy7PE and Cy7APC: Bright new probes for immunofluorescence. Cytometry 24:191–197, 1996.
24. Roederer M, Murphy RF: Cell-by-cell autofluorescence correction for low signal-to-noise systems: Application to epidermal growth factor endocytosis by 3T3 fibroblasts. Cytometry 7:558–565, 1986.
25. Rolink A, ten Boekel E, Melchers F, Fearon DT, Krop I, Andersson J: A subpopulation of B220+ cells in murine bone marrow does not express CD19 and contains natural killer cell progenitors. J Exp Med 183:187–194, 1996.
26. Sanders ME, Makgoba MW, Shaw S: Human naive and memory T cells. Immunol Today 9:195–199, 1988.
27. Watanabe N, Rosa SCD, Cmelak A, Hoppe R, Herzenberg LA, Herzenberg LA, Roederer M: Long-term depletion of naive T cells in patients treated for Hodgkin's disease. Blood, in press (1997).